DOI: 10.1017/cjn.2024.328
This is a manuscript accepted for publication in *Canadian Journal of Neurological Sciences*.
This version may be subject to change during the production process.

Imaging for management of chronic Subdural Hematoma- a review

Sandeep Devgan,[1] MD, Dr. Jai Shankar[1] MD, DM, MSc, FRCPC

[1]Department of Radiology, University of Manitoba, Winnipeg, Manitoba, Canada.

Conflicts of Interest: The authors have no conflicts of interest to declare. Dr Jai Shankar is the PI for EMMA Can study which is a randomized control trial for EMMA for Chronic subdural hematoma in Canada.

Sources of Funding: No funding was received for this research.

Short Title: Imaging for chronic subdural hematoma management

E-mails:
Sandeep Devgan, Email- devgans@myumanitoba.ca
Dr. Jai Shankar, Email- shivajai1@gmail.com

Corresponding Author: Dr. Jai Shankar MD, DM, MSc, Diagnostic and interventional neuroradiologist and Professor of Radiology, Department of Radiology, University of Manitoba, Winnipeg, Manitoba, Canada, Email: shivajai1@gmail.com

ABSTRACT:

Radiologic imaging has become integral in not only the detection and diagnosis of subdural hematoma (SDH), but also in guiding potential treatment options. Particularly, in the arena of chronic SDH, which has conventionally been managed via surgical drainage, although is shifting toward intervention with embolization of the middle meningeal artery (MMA). We review the imaging manifestations of SDH as a function of chronicity, standardized methods of measurement, and identify the MMA and its clinically significant variant anatomy as it pertains to embolization planning. Equipped with a more comprehensive approach to characterizing SDH, the radiologist will be able to curate findings of greater utility to the clinician.

Summary points-

- Highlights the imaging characterization of subdural hematoma (SDH) in the era of embolization of middle meningeal artery (EMMA) as well as the surgical drainage for chronic SDH.
- Highlights the characterization of chronic or non-acute SDH and its size assessment.
- Identifying the anatomy of middle meningeal artery (MMA) on CT angiography.

https://doi.org/10.1017/cjn.2024.328 Published online by Cambridge University Press

INTRODUCTION:

Subdural hematoma (SDH) is a collection of blood products between the dura and arachnoid meninges, which surround the brain parenchyma. The dura mater is the outermost layer of the meninges and is continuous with periosteum of the skull. The dura reflects along the midline, where the two cerebral hemispheres adjoin, to form the cerebral falx. The dura is also reflected along the inferior surface of the cerebral hemispheres and superior surface of the cerebellar hemispheres to form the tentorial leaflets. The dural venous sinuses are contained within these reflections. Cortical veins drain into the dural venous sinuses by traversing across the subdural space, and SDH is conventionally thought to result from tearing of these bridging veins[1].

However, in the setting of chronic SDH (cSDH), trauma may actually play a minor or absent role. Instead, cSDH development and progression is posited to be driven foremost by inflammation. The dura is lined with a layer of connective tissue cells termed dural border cells, and damage to these border cells may initiate a sustained inflammatory response, resulting in neomembrane formation and fluid accumulation[2].

Although surgical evacuation has conventionally been the management of cSDH, given the underlying inflammatory pathophysiology, there has been a shift toward embolization of the middle meningeal artery (EMMA) as a potential therapeutic option, as it may theoretically decrease neovascularity, and therefore inflammation within the subdural space (figure 1).

Radiologic outcomes will be a cornerstone for any future trial looking to compare the efficacy of EMMA with surgical drainage. However, for there to be any meaningful comparison either within a trial or between trials, there must be a standardized approach to interpreting imaging. The purpose of this paper is then to review the literature for different approaches to characterizing SDH, review pertinent anatomy of the MMA , and highlight the importance of neck imaging for therapeutic planning.

GENERAL ANATOMY AND APPEARANCE:

Knowledge of the anatomy of the subdural space aids in understanding the imaging morphology of SDH. Classically, SDH appears as a concavo-convex, or crescentic, extra-axial collection overlying the cerebral convexities. Because of the dural reflections, SDH rarely crosses the midline. However, SDH can collect along the cerebral falx or tentorial leaflets.

https://doi.org/10.1017/cjn.2024.328 Published online by Cambridge University Press

Unlike epidural hematoma, SDH can cross suture lines because only the dura mater, and not the underlying arachnoid mater, is adherent to the calvarium at the sutures[1].

The chronicity of SDH can be ascertained by the radiodensity of blood products measured in Hounsfield units (HU). The general trend is a decrease in radiodensity of blood products overtime with an estimated decrease of approximately 1.5 HU per day[1,4,5] (Figure 2).

ACUTE SUBDURAL HEMATOMA:

Acute SDH (aSDH) is characterized by blood products zero to several days in age. The majority of aSDH (60%) are hyperdense when compared to the brain parenchyma, with attenuation ranging from 50 to 80 HU. The remainder of aSDH (40%) demonstrate mixed hyperdensity and hypodensity[6]. The hypodensity may relate to unclotted blood products, CSF leakage through torn arachnoid membranes, or severe anemia[7]. In fact, a "swirl sign", where there are hypodense pockets in a predominately hyperdense collection, has been associated with active extravasation of unclotted blood[8].

SUBACUTE SUBDURAL HEMATOMA:

Subacute SDH is characterized by blood products approximately several days to a few weeks in age. In the subacute stage, hematoma begins to organize with hemoglobin degradation and neomembrane formation. New or recurrent hemorrhage may relate to bleeding from bridging cortical veins, or friable neomembranes[1].

Although the distribution of hematoma is similar, the collection becomes progressively hypodense. In the absence of new hemorrhage, the collection becomes isodense with adjacent brain parenchyma, typically within 10 - 14 days. As a result, subtle signs of mass effect, such as sulcal or ventricular effacement, may be the only clues to suggest presence of subacute SDH. However, subacute SDH often demonstrate mixed attenuation as blood products are in various stages of degradation. As a result, there is a subtle hematocrit gradient with more hyperdense blood product layering dependently within the hematoma[1,5].

CHRONIC SUBDURAL HEMATOMA:

cSDH is characterized by blood products greater than 2 to 3 weeks in age. As blood products continue to degrade, there is progressive liquifecation of the hematoma, and formation

https://doi.org/10.1017/cjn.2024.328 Published online by Cambridge University Press

of a fibrous capsule. In the absence of new hemorrhage, cSDH is usually homogeneously hypodense, although may also demonstrate a subtle hematocrit gradient[1].

cSDH may develop internal septations, which can appear hyperdense. The fibrous capsule may also appear hyperdense, becoming thickened and coarsely calcified over time[5,6].

The appearance of a homogeneously hypodense cSDH may be indistinguishable from a subdural hygroma, which is a sudural collection of CSF as a result of traumatic arachnoid tearing, passive effusion in setting of spontaneous intracranial hypotension, dehydration, or brain atrophy. The only distinguishing factor may be prior imaging demonstrating subdural blood products[1].

Additionally, cSDH and subdural hygroma may be difficult to distinguish from prominent extra-axial CSF spaces secondary to brain volume loss. In the setting of severe volume loss, a large volume of subdural hemorrhage or CSF can be accommodated without signs of mass effect. The presence of cortical vessels traversing the extra-axial space favours volume loss, as these would be displaced in the setting of a subdural collection[5,9].

ACUTE ON CHRONIC SUBDURAL HEMATOMA:

Heterogeneity within SDH may relate to acute hemorrhage into an existing cSDH. This was again conventionally thought to result from tearing of bridging cortical veins, although now thought to be secondary to an underlying inflammatory process with formation of new “leaky” blood vessels, which allow for microhemorrhages. Different from the subtle hematocrit gradient, is a more distinct layering of acute hyperdense blood products dependently resulting in a “fluid-fluid” level. Acute hyperdense blood products may also be scattered, or more compartmentalized and appear loculated[10].

NON-ACUTE SUBDURAL HEMATOMA:

There is significant variation in the reported incidence of cSDH, ranging from 1.72 - 20.6 per 100,000 persons per year. Although some of this variation can be attributed to geographic differences, an aging population, and increasing uptake of antithrombotic medications, part of it may relate to a lack of standardized imaging parameters for characterizing cSDH[11]. Instead, SDH may be classified as acute or non-acute, where non-acute SDH is constituted by more than 50%

https://doi.org/10.1017/cjn.2024.328 Published online by Cambridge University Press

of the total hematoma volume being iso or hypodense to the brain parenchyma on non-contrast CT[12].

MEASURING CHRONIC SUBDURAL HEMATOMA:

Accurate and reproducible measurements of SDH is crucial for not only conveying a sense of magnitude, but also in monitoring the evolution of hematoma, particularly when evaluating treatment response. Although no standardized approach exists, there are a few commonly employed techniques for measuring SDH .

Width: The simplest parameter to measure is width. The width of a hematoma is measured perpendicular to the inner table of the calvarium (Figure 3a). On axial images, caution must be applied above the level of the superior temporal line, as slices are no longer perpendicular to the calvarium, but rather oblique due to the curvature of the cranial vault (Figure 3b). As a result, the use of coronal reformats may be helpful[13] (Figure 3c).

Volume: Volume of hematoma is best evaluated using multiplanar reformats. Volume can be estimated using the formula V = ABC/2, which approximates the volume of half an ellipsoid, where A, B, and C correspond to the perpendicular measurements of length, width, and height of hematoma[14-17] (figure 4). The input for A, B, and C should represent the corresponding maximum values, which may not be on the same image slice[15]. Height may be measured by multiplying the number of axial slices with visible hematoma by the slice thickness[14-16].

Midline Shift: Due to the closed nature of the cranium, the space occupying effect of SDH often results in sulcal effacement and compression of the CSF spaces. The degree of space occupying effect can be conveyed by measuring the midline shift (MLS). A few techniques for estimating MLS exist.

One method for estimating MLS involves measuring the inner diameter of the skull (a), followed by measuring the distance from the inner table of the skull to the septum pellucidum contralateral to the hematoma at the same level (b). MLS can be estimated by the formula: MLS = (a/2) - b[18] (Figure 5a).

Given the potential for skull asymmetry and patient misalignment in the scanner, another widely adopted method includes estimating MLS from the ideal midline (iML), which is a line drawn between the anterior and posterior points of the visible falx. MLS is then calculated

https://doi.org/10.1017/cjn.2024.328 Published online by Cambridge University Press

as the distance perpendicular to the iML extending to the farthest point of the displaced septum pellucidum[18] (Figure 5b).

Both of these methods can be employed at various fixed locations, such as at the level of the foramen of Monro, thalamus, and mid-septum pellucidum, or simply at the level where there is maximal displacement of the septum pellucidum. Overall, the method employing ideal midline (iML) may provide greater inter-rater concordance[19].

FOLLOW-UP IMAGING:

There are a few limitations to accurately measuring SDH, which makes assessment for progression on subsequent imaging challenging. As mentioned previously, above the level of the superior temporal line axial slices are no longer perpendicular to the calvarium due to the curvature of the cranial vault. A similar obstacle arises when attempting to measure subtentorial hematoma[13,16].

Measuring MLS is complicated in the scenario of bilateral SDH, where mass effect from opposing hematoma may balance one another out[20,21,22]. Similarly, MLS may be minimal in the scenario of advanced brain parenchymal atrophy, where the subdural space is able to accommodate a large volume of hematoma with negligible MLS [1,23].

Additionally, as the shape of hematoma deviates from the ideal half-ellipsoid shape, becoming lenticular or even loculated, assessment of total volume becomes less accurate[22] (Figure 6).

Although laborious, measuring SDH volume on follow-up imaging is intuitively the most accurate as it attempts to quantify hematoma in multiple planes. However, further research is required for validation. In the absence of any further evidence, ongoing clinical trials on the cSDH should standardize measurement criteria on initial imaging, and implement the same criteria on follow-up imaging for ideal comparison. Using multiple measurement methods in future studies will aid in determining the most optimum technique to employ in the clinical setting.

NEUROANGIOGENESIS:

One of the key issues with cSDH is recurrence. The rate of recurrence ranges from 7.5 - 29%, with greater than 90% within 2 months of the initial surgery[24]. Recurrence is more likely

https://doi.org/10.1017/cjn.2024.328 Published online by Cambridge University Press

with bilateral hematoma, significant brain atrophy, and anticoagulation[25,26]. Reoperation is often complicated by an older and comorbid demographic[25]. The treatment cost associated with recurrent cSDH may be 132% greater than non-recurrent treatment cost[27].

Although conventionally thought of as sequela of trauma, propagation of cSDH may instead largely be facilitated by a cascade of inflammation, angiogenesis of fragile vessels, and ultimately, hemorrhage[2]. Radiologically, inflammation and neovascularity manifests as an increase in the median diameter of the MMA ipsilateral to a cSDH[28]. Additionally, on conventional angiogram, regions of contrast blush are thought to represent ongoing leakage or micro-hemorrhage. Because pathophysiology dictates management, EMMA attempts to reduce the degree of neovascularity, thereby decreasing the volume of cSDH and reducing the risk of recurrence.

IMAGING FINDINGS OF MIDDLE MENINGEAL ARTERY:

With the increasing use of EMMA for management of cSDH , the knowledge of anatomy of the MMA for guiding neurointerventional management is paramount[29]. Although digital subtraction angiography remains the gold standard for delineating the MMA, CT angiography (CTA) is being increasingly used for planning of EMMA. The advances in multidector CT imaging allows for identification on most thin-section CT angiogram protocols. Despite this, identification of the normal calibre MMA is not routine practice, as it is relatively small in caliber, and there is a lack of emphasis on its significance within the current literature.

NORMAL ANATOMY:

The external carotid artery (ECA) has 8 major branches, of which the two terminal branches include the superficial temporal artery and the internal maxillary artery (IMAX). The IMAX is the larger of the two terminal branches and gives rise to the MMA as its first major branch. The MMA courses superiorly through the foramen spinosum to supply the cranial meninges[30]. On axial images, it can be seen anterolateral to the internal carotid artery (ICA) just below the level of the skull base (Figure 7). Although pertinent, the variant anatomy of MMA is not very well seen on CTA. With more experience on CTA for identifying MMA, we will be able to identify the variant anatomy of MMA. Identifying these variants is crucial for keeping the

https://doi.org/10.1017/cjn.2024.328 Published online by Cambridge University Press

procedure of EMMA safe as well as giving a very good idea about the technical feasibility of EMMA.

VARIANT ANATOMY:

There are multiple clinically significant variants of MMA anatomy, including communications to a few important vessels, such as the ophthalmic, internal carotid, ascending pharyngeal, and occipital arteries. These communications may serve as useful treatment routes, or be characterized as "dangerous anastomoses" when considering interventions such as embolization[31].

Accessory Meningeal Supply of the MMA: The accessory meningeal artery is usually a branch from the IMAX, although can also arise from the MMA. It enters the skull via the foramen ovale, where it can have multiple intracranial anastomoses, including with the MMA. In fact, it can supply the MMA to varying degrees, ranging from supply of the frontal and petrous branches of the MMA to complete supply of the MMA[31].

Orbital anastomoses and Variants: The MMA has multiple communications within the orbit, which exist on a spectrum, such that the connections may be small or large. When the anastomoses are prominent, the MMA may become the primary supply of the orbit, or vice-versa[31].

When the MMA has a conventional origin from the IMAX, communication with orbital vessels occurs via the sphenoid branch of the MMA. The communicating vessels travel along the sphenoid ridge to enter the orbit via the superior orbital fissure (SOF) and/or foramen of Hyrtl laterally[31].

Meningo-opthalmic Variant: Conventionally, supply of orbit occurs via the ophthalmic artery, a branch arising from the supraclinoid ICA anteriorly. In this variant, the orbit is completely supplied by the MMA via the anastomoses of the sphenoid branch of the MMA and ophthalmic artery, termed the meningo-opthalmic artery, which enters the orbit via the SOF[31].

Meningo-lacrimal Variant: Partial supply restricted to the lateral orbit and lacrimal gland by the MMA can occur via anastomoses of the sphenoid branch of the MMA and lacrimal branch of the ophthalmic artery, which enters the orbit via the foramen of Hyrtl[31].

https://doi.org/10.1017/cjn.2024.328 Published online by Cambridge University Press

Recurrent Meningeal Variant: At the other end of the spectrum, a more common variant is supply of the MMA from the ophthalmic artery. The degree of supply also exists on a continuum, whereby supply from the ophthalmic artery may be restricted to a single MMA territory, while the remainder is supplied via the conventional IMAX pathway[31] (Figure 8 and Figure 9).

IMAGING OF THE NECK:

A comprehensive workup for potential therapeutic embolization for SDH must include arterial imaging of the neck. A survey of the neck vessels to delineate tortuosity, atherosclerotic disease, and aberrant anatomy provides a roadmap for vascular access planning. Imaging of neck is particularly important as patients of cSDH are usually older and could potentially have other vascular comorbidities (Figure 10).

CONCLUSION:

Attempts at characterizing the chronicity of SDH based on time course since onset is complicated by not only a lack of a time-based consensus within the literature, but also in the scenario where the initial time of onset is not known, and imaging must be interpreted without the benefit of chronology. Instead, having an imaging consensus of acute vs non-acute SDH based on attenuation characteristics may promote uniformity within the literature. Similarly, future trials should standardize the measurement protocol on the initial imaging and utilize the same approach on subsequent follow-up for consistency. The use of multiple measurement methods may lead to the validation of the less cumbersome methods, which may be more clinically feasible.

It is important to recognize the normal origin of the MMA on CTA, particularly as it traverses through the foramen spinosum. If normal origin of MMA on CTA is not identified, attempt at EMMA may not be undertaken, regardless of the variant anatomy. Similar to stroke patients, extension of the CTA to include the neck vessels is paramount for vascular access planning.

Statement of authorship- SD wrote the first draft of the manuscript. JS conceptualized the project and reviewed the final draft of the manuscript.

https://doi.org/10.1017/cjn.2024.328 Published online by Cambridge University Press

REFERENCE:

1. Carroll JJ, Lavine SD, Meyers PM. Imaging of Subdural Hematomas. Neurosurg Clin N Am. 2017;28(2):179-203. doi:10.1016/j.nec.2016.11.001
2. Edlmann E, Giorgi-Coll S, Whitfield PC, Carpenter KLH, Hutchinson PJ. Pathophysiology of chronic subdural haematoma: Inflammation, angiogenesis and implications for pharmacotherapy. J Neuroinflammation. 2017;14(1):1-13. doi:10.1186/s12974-017-0881-y
3. Avis S. Nontraumatic Acute Subdural Hematoma A Case Report and Review of the Literature. Am J Forensic Med Pathol. 1993;14(2):130-134.
4. Scotti G, Terbrugge K, Melancon D, Belanger G. Evaluation of the age of subdural hematomas by computerized tomography. J Neurosurg. 1977;47(3):311-315. doi:10.3171/jns.1977.47.3.0311
5. Lee KS, Bae WK, Bae HG, Doh JW, Yun IG. The computed tomographic attenuation and the age of subdural hematomas. J Korean Med Sci. 1997;12(4):353-359. doi:10.3346/jkms.1997.12.4.353
6. Rincon S, Gupta R, Ptak T. Chapter 22 - Imaging of head trauma. In: Masdeu JC, González RGBT-H of CN, eds. Neuroimaging Part I. Vol 135. Elsevier; 2016:447-477. doi:https://doi.org/10.1016/B978-0-444-53485-9.00022-2
7. Reed D, Robertson WD, Graeb DA, Lapointe JS, Nugent RA, Woodhurst WB. Acute subdural hematomas: Atypical CT findings. Am J Neuroradiol. 1986;7(3):417-421.
8. Al-Nakshabandi NA. The Swirl Sign. Radiology. 2001;218(2):433. doi:10.1148/radiology.218.2.r01fe09433
9. Markwalder TM. Chronic subdural hematomas: a review. J Neurosurg. 1981;54(5):637-645. doi:10.3171/jns.1981.54.5.0637
10. Tan S, Aronowitz P. Hematocrit effect in bilateral subdural hematomas. J Gen Intern Med. 2013;28(2):321. doi:10.1007/s11606-012-2179-1
11. Yang W, Huang J. Chronic Subdural Hematoma: Epidemiology and Natural History. Neurosurg Clin N Am. 2017;28(2):205-210. doi:10.1016/j.nec.2016.11.002
12. Hutchinson PJ, Edlmann E, Bulters D, et al. Trial of Dexamethasone for Chronic Subdural Hematoma. N Engl J Med. 2020;383(27):2616-2627. doi:10.1056/nejmoa2020473

13. Mcdonough R, Bechstein M, Fiehler J, et al. Radiologic Evaluation Criteria for Chronic Subdural Hematomas: Recommendations for Clinical Trials. Am J Neuroradiol. 2022;43(11):1550-1558. doi:10.3174/ajnr.A7503
14. Gebel JM, Sila CA, Sloan MA, et al. Comparison of the ABC/2 estimation technique to computer-assisted volumetric analysis of intraparenchymal and subdural hematomas complicating the GUSTO-1 trial. Stroke. 1998;29(9):1799-1801. doi:10.1161/01.STR.29.9.1799
15. Won SY, Zagorcic A, Dubinski D, et al. Excellent accuracy of ABC/2 volume formula compared to computer-assisted volumetric analysis of subdural hematomas. PLoS One. 2018;13(6):1-6. doi:10.1371/journal.pone.0199809
16. Sucu HK, Gokmen M, Gelal F. The value of XYZ/2 technique compared with computer-assisted volumetric analysis to estimate the volume of chronic subdural hematoma. Stroke. 2005;36(5):998-1000. doi:10.1161/01.STR.0000162714.46038.0f
17. Kothari RU, Brott T, Broderick JP, et al. The ABCs of measuring intracerebral hemorrhage volumes. Stroke. 1996;27(8):1304-1305. doi:10.1161/01.STR.27.8.1304
18. Liao CC, Chen YF, Xiao F. Brain midline shift measurement and its automation: A review of techniques and algorithms. Int J Biomed Imaging. 2018;2018. doi:10.1155/2018/4303161
19. Zanolini U, Austein F, Fiehler J, et al. Midline Shift in Chronic Subdural Hematoma: Interrater Reliability of Different Measuring Methods and Implications for Standardized Rating in Embolization Trials. Clin Neuroradiol. 2022;32(4):931-938. doi:10.1007/s00062-022-01162-1
20. Juković MF, Stojanović DB. Midline shift threshold value for hemiparesis in chronic subdural hematoma. Srp Arh Celok Lek. 2015;143(7-8):386-390. doi:10.2298/SARH1508386J
21. Hsieh CT, Su IC, Hsu SK, Huang CT, Lian FJ, Chang CJ. Chronic subdural hematoma: Differences between unilateral and bilateral occurrence. J Clin Neurosci. 2016;34:252-258. doi:10.1016/j.jocn.2016.09.015
22. Bechstein M, McDonough R, Fiehler J, et al. Radiological Evaluation Criteria for Chronic Subdural Hematomas: Review of the Literature. Clin Neuroradiol. 2022;32(4):923-929. doi:10.1007/s00062-022-01138-1

23. Gelabert-González M, Iglesias-Pais M, García-Allut A, Martínez-Rumbo R. Chronic subdural haematoma: Surgical treatment and outcome in 1000 cases. Clin Neurol Neurosurg. 2005;107(3):223-229. doi:10.1016/j.clineuro.2004.09.015
24. Atefi N, Alcock S, Silvaggio JA, Shankar J. Clinical Outcome and Recurrence Risk of Chronic Subdural Hematoma After Surgical Drainage. Cureus. 2023;15(2):35525. doi:10.7759/cureus.35525
25. Schwarz F, Loos F, Dünisch P, et al. Risk factors for reoperation after initial burr hole trephination in chronic subdural hematomas. Clin Neurol Neurosurg. 2015;138:66-71. doi:10.1016/j.clineuro.2015.08.002
26. Oishi M, Toyama M, Tamatani S, Kitazawa T, Saito M. Clinical factors of recurrent chronic subdural hematoma. Neurol Med Chir (Tokyo). 2001;41(8):382-386. doi:10.2176/nmc.41.382
27. Rauhala M, Helén P, Huhtala H, et al. Chronic subdural hematoma—incidence, complications, and financial impact. Acta Neurochir (Wien). 2020;162(9):2033-2043. doi:10.1007/s00701-020-04398-3
28. Pouvelle A, Pouliquen G, Premat K, et al. Larger Middle Meningeal Arteries on Computed Tomography Angiography in Patients with Chronic Subdural Hematomas as Compared with Matched Controls. J Neurotrauma. 2020;37(24):2703-2708. doi:10.1089/neu.2020.7168
29. Link TW, Boddu S, Paine SM, Kamel H, Knopman J. Middle Meningeal Artery Embolization for Chronic Subdural Hematoma: A Series of 60 Cases. Neurosurgery. 2019;85(6):801-807. doi:10.1093/neuros/nyy521
30. Osborn, A. G., Salzman, K. L., Hedlund GL. Osborn's Brain: Imaging, Pathology, and Anatomy.; 2017.
31. Neuroangio. http://neuroangio.org/anatomy-and-variants/middle-meningeal-artery/. Published 2023.

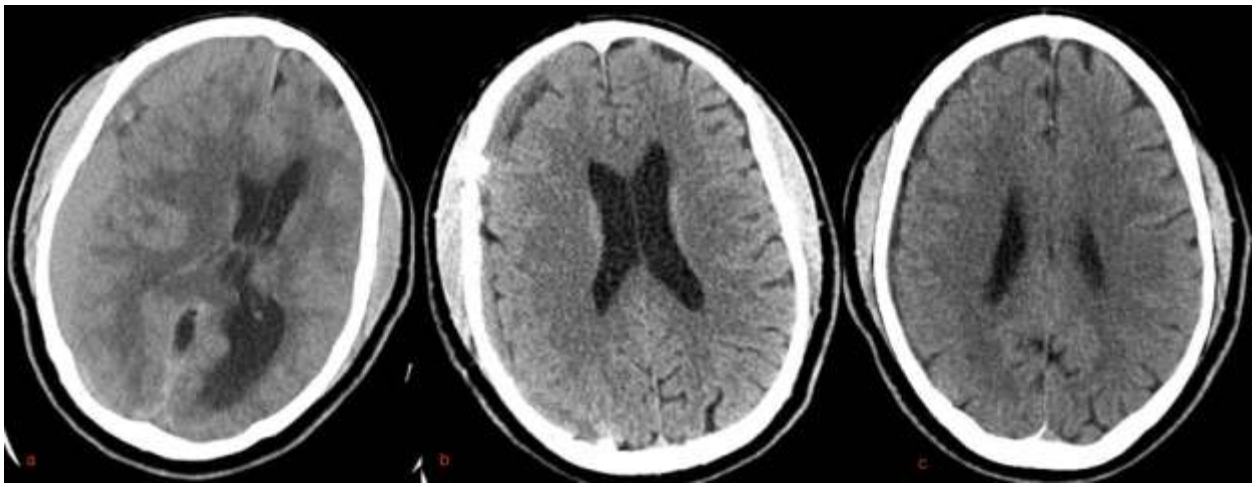

Figure 1: Follow up of SDH following surgical evacuation and EMMA: (a) Non-contrast CT head demonstrating large right convexity SDH, which is largely isodense/hyperdense to brain parenchyma, although contains some hypodensity, suggestive of possible non-acute component. (b) Non-contrast CT head 2 months following surgical evacuation and EMMA demonstrates expected evolution of SDH, which appears smaller and more hypodense. (c) Non-contrast CT head 8 months following surgical evacuation and EMMA demonstrating further interval improvement with only thin residual hypodense SDH and no evidence of recurrent SDH.

https://doi.org/10.1017/cjn.2024.328 Published online by Cambridge University Press

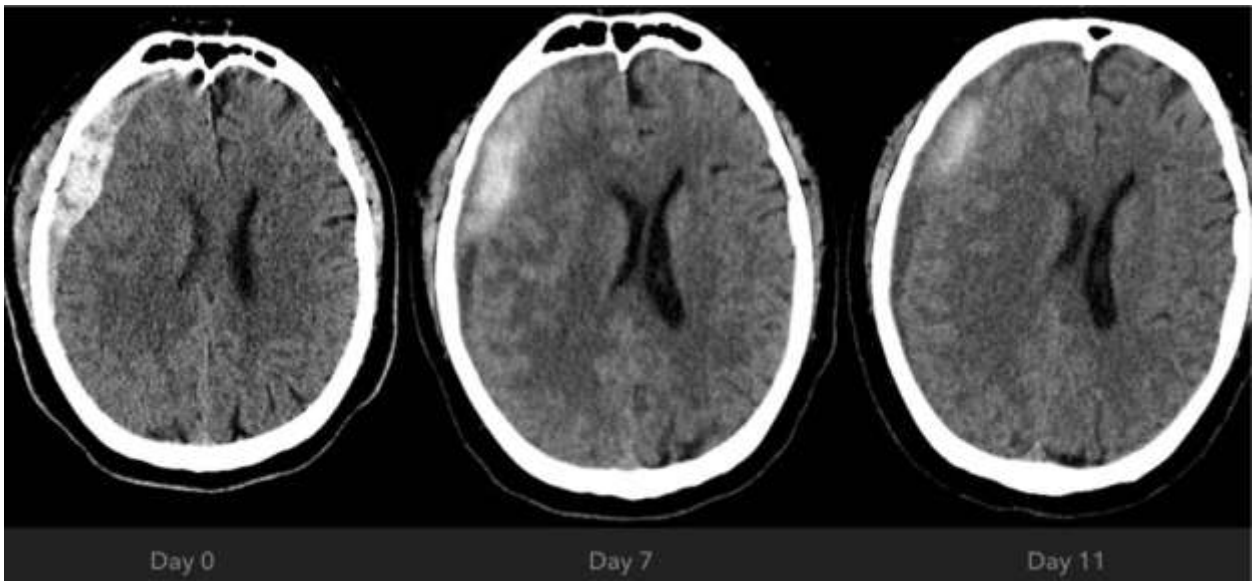

Figure 2: From left to right: Axial non-contrast imaging of the brain day 0,7, and 11 from onset of subdural hematoma (SDH). Note general decrease in attenuation of SDH with time since onset.

https://doi.org/10.1017/cjn.2024.328 Published online by Cambridge University Press

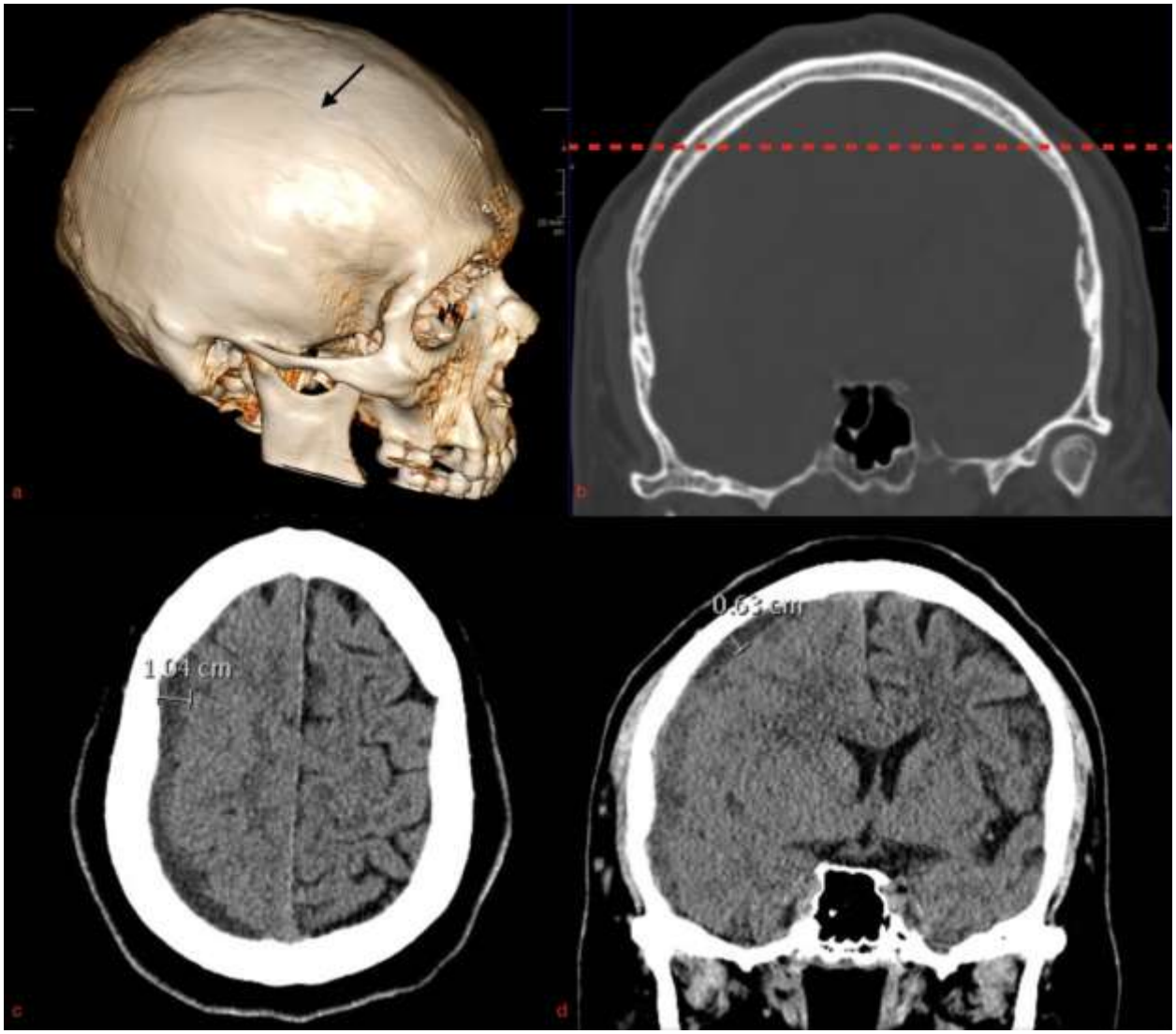

Figure 3: Pitfalls of measuring SDH width: (a) 3D reconstruction demonstrating superior temporal line (black arrow), which is a bony ridge arising from the zygomatic process of the frontal bone, and serves as the attachment of the temporal fascia. (b) Coronal CT head on bone window at the level of the superior temporal line (dotted red line). (c) Attempting to measure SDH width on an axial image above the superior temporal line may result in overestimation. (d) As a result, above the superior temporal line, SDH width measurements perpendicular to the inner table of the calvarium on coronal reformats may be more accurate and reproducible.

https://doi.org/10.1017/cjn.2024.328 Published online by Cambridge University Press

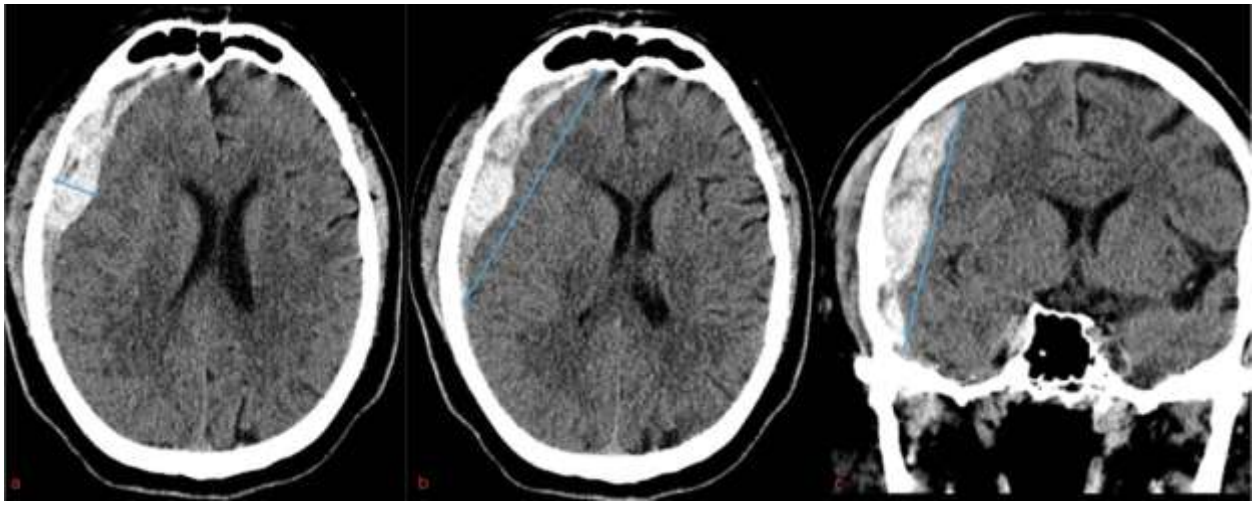

Figure 4: Manual measurement of SDH volume as given by half-ellipsoid volume formula V = ABC/2, where V (volume), A (width), B (length), and C (height). Measurement (solid blue line) of SDH width (a), length (b), and height (c). Values of A, B, and C should be perpendicular to each other and represent the maximum values, which may not be on the same slice. Alternatively, SDH height (C) may be calculated by the product of slice thickness and the number of slices where SDH is visible.

https://doi.org/10.1017/cjn.2024.328 Published online by Cambridge University Press

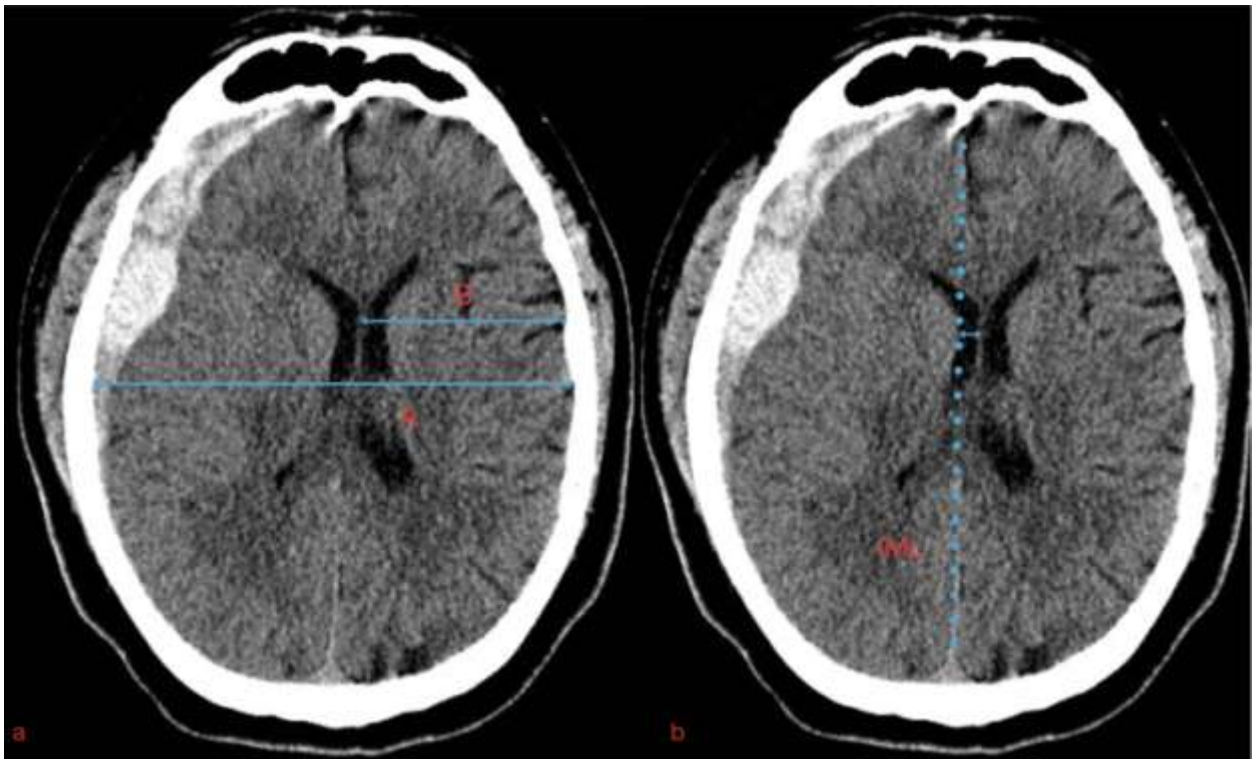

Figure 5: Methods for measuring midline shift (MLS): (a) Given by formula MLS = (A/2) - B, where (A) is the inner diameter of the skull, and (B) is distance from the inner table of the skull to the septum pellucidum contralateral to the hematoma at the same level. (b) Ideal midline (iML) is drawn between the anterior and posterior points of the visible falx. MLS is then calculated as the distance perpendicular to the iML extending to the farthest point of the displaced septum pellucidum.

https://doi.org/10.1017/cjn.2024.328 Published online by Cambridge University Press

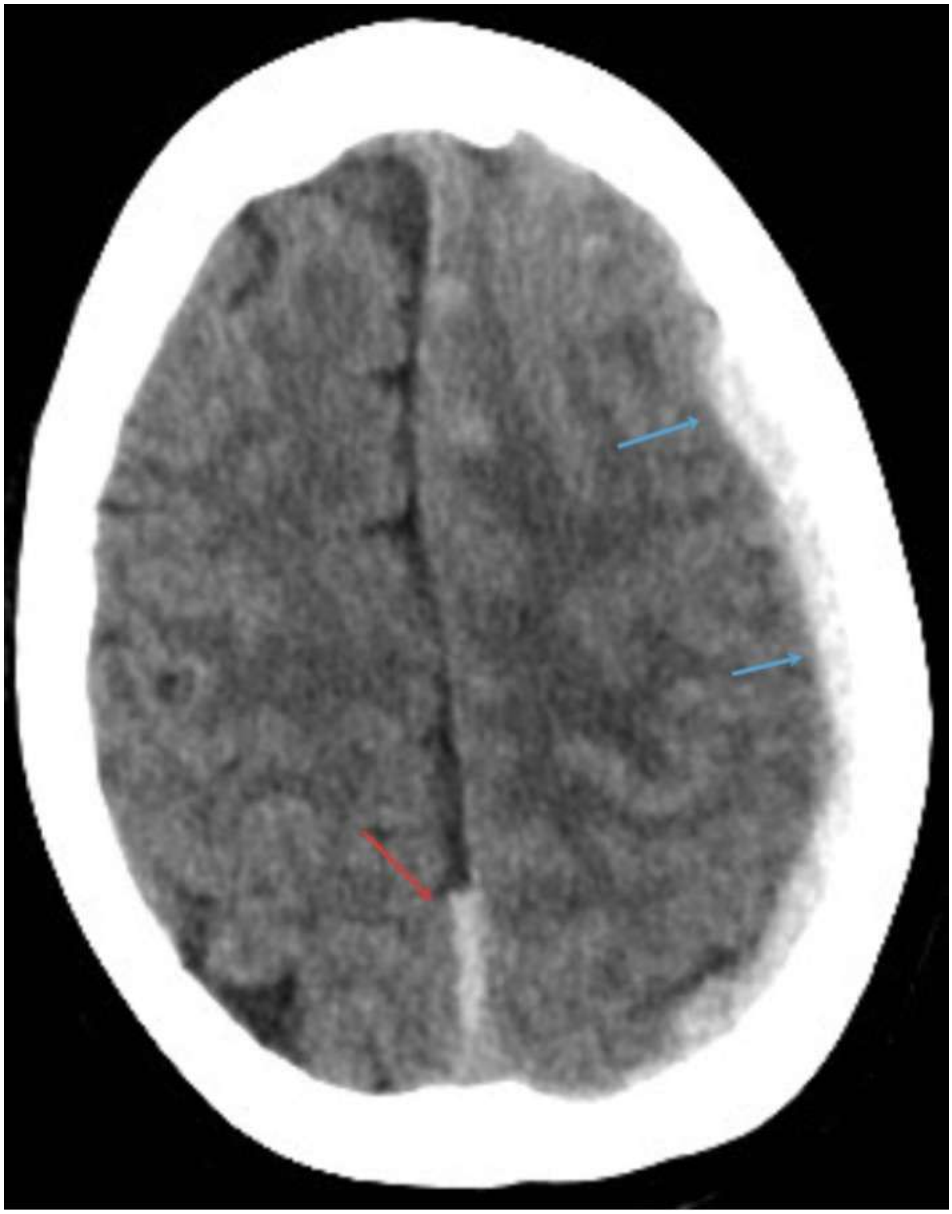

Figure 6: Pitfalls of measuring SDH volume: As SDH shape deviates from the ideal half-ellipsoid shape, becoming locualted or tracking along the falx, the formula to estimate SDH volume becomes less accurate. More conventionally shaped crescentic (blue arrows) vs. Posterior falx SDH (red arrow).

https://doi.org/10.1017/cjn.2024.328 Published online by Cambridge University Press

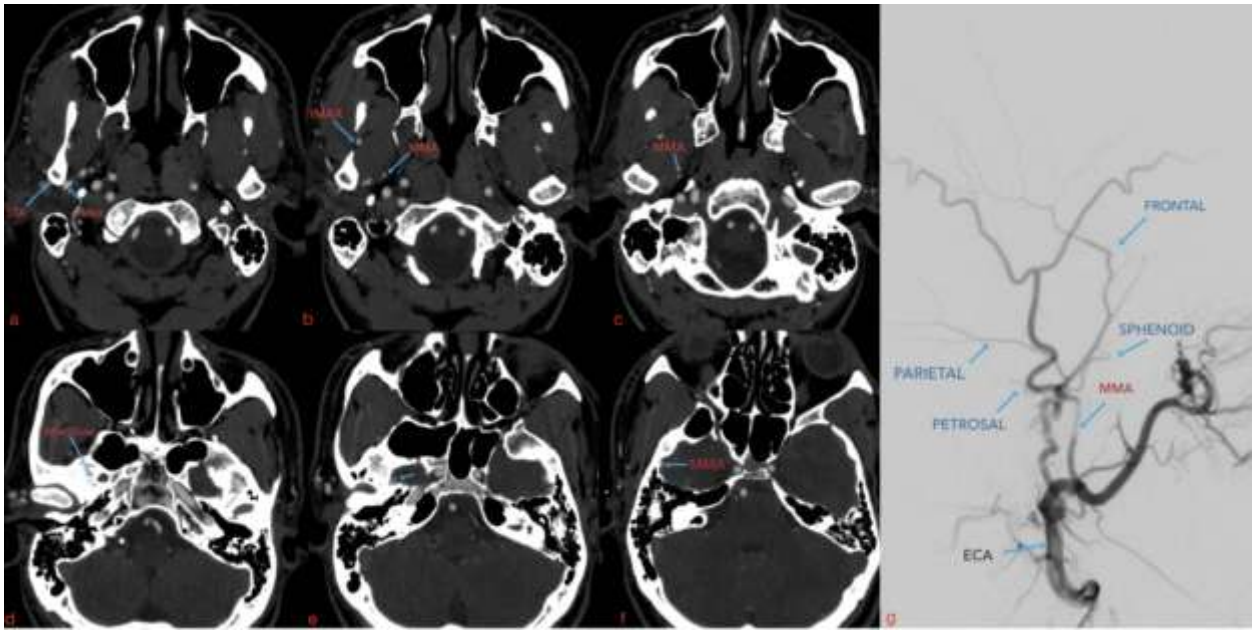

Figure 7: Normal MMA anatomy: On CTA (a - f), inferior to superior axial images at the level of the skull base demonstrating termination of the external carotid artery (ECA) into the superficial temporal artery (STA) and internal maxillary artery (IMAX). The middle meningeal artery (MMA) is conventionally the 1st branch of the IMAX and travels through the foramen spinosum to enter the cranial vault. On DSA (g), the ECA terminates into the STA and IMAX. The MMA is conventionally the 1st branch from the IMAX. The MMA gives rise to multiple branches, including parietal, petrosal, frontal, and sphenoid.

https://doi.org/10.1017/cjn.2024.328 Published online by Cambridge University Press

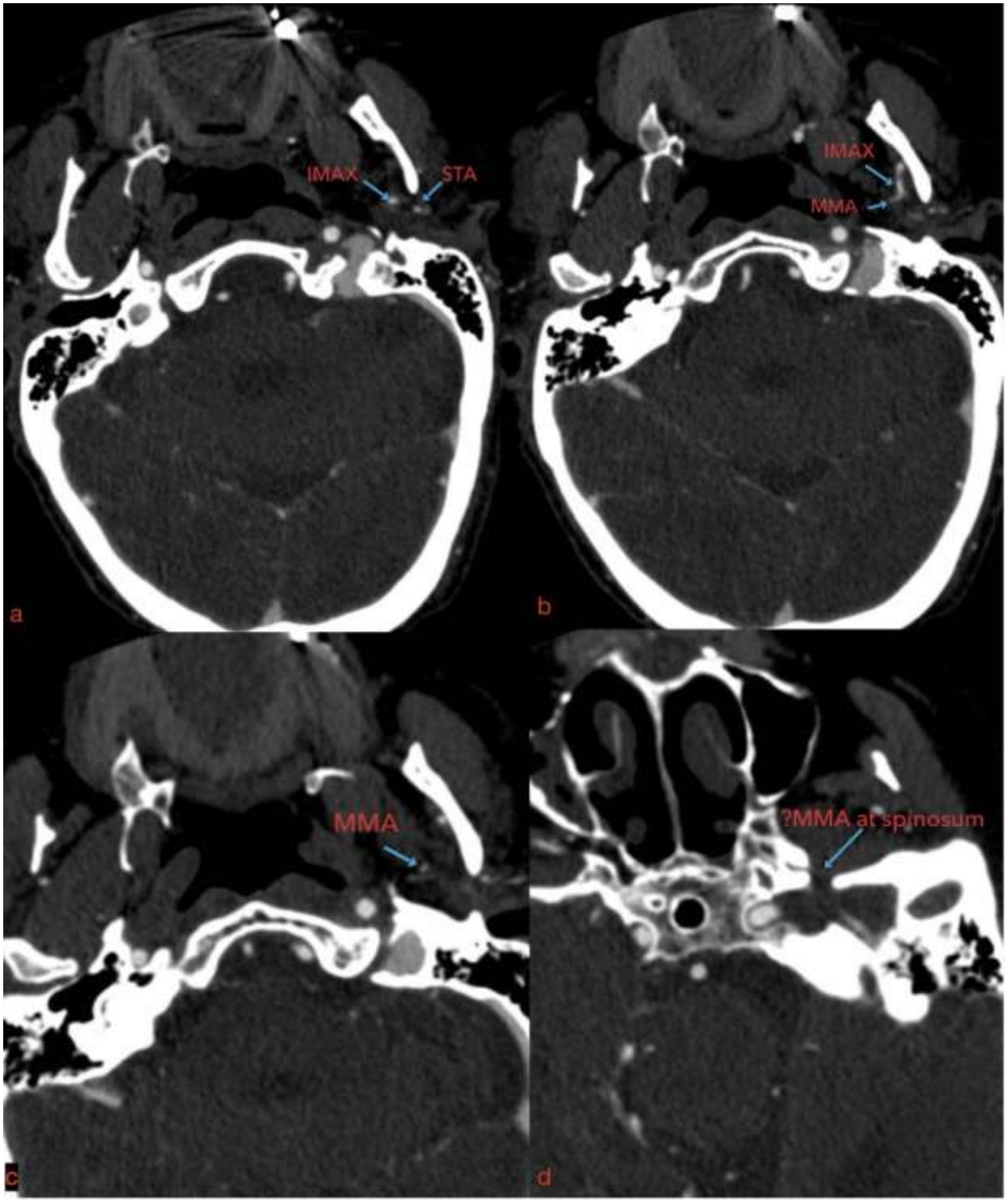

Figure 8: Case of aberrant MMA anatomy: (a - d) Inferior to superior axial CTA images at the level of the skull base demonstrating MMA origin and course through the foramen spinosum on the right. However, expected origin of the MMA on the left is absent, suggestive of aberrant supply.

https://doi.org/10.1017/cjn.2024.328 Published online by Cambridge University Press

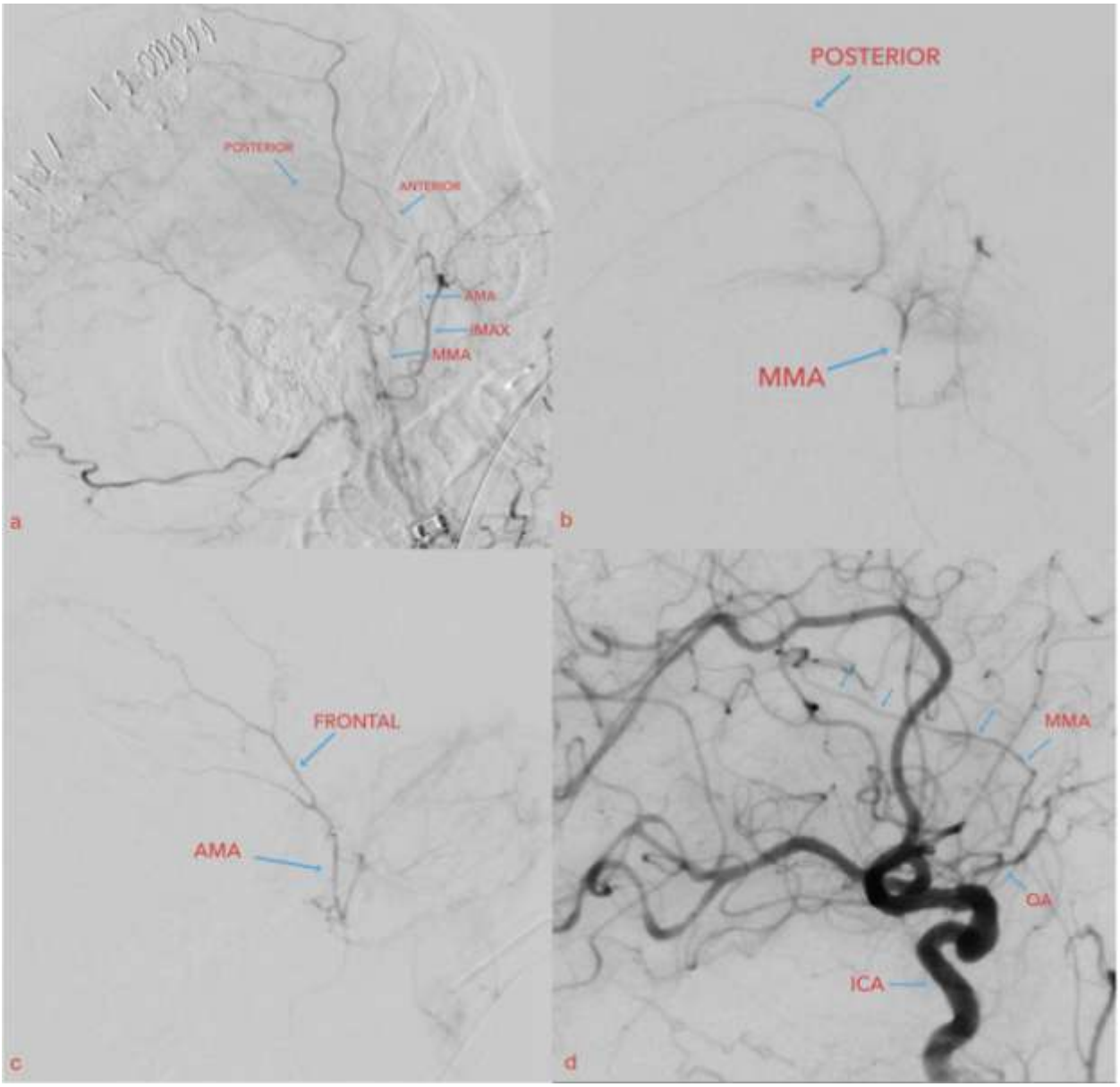

Figure 9: Case of aberrant MMA anatomy: (a) Patient subsequently underwent conventional DSA of the ECA, which failed to demonstrate conventional origin of the MMA from the IMAX. (b) Conventional DSA of the ICA demonstrated supply of the MMA entirely from the ophthalmic artery (OA), also known as recurrent meningeal variant. As a result, patient was not a candidate for EMMA. (c - e) Inferior to superior CTA axial images at the level of the orbits. In retrospect, the OA supplying the sphenoid branch of the MMA can be seen on the CTA, although would have been difficult to definitively call prospectively.

https://doi.org/10.1017/cjn.2024.328 Published online by Cambridge University Press

Figure 10: (a) Sagittal reformat of CTA aortic arch and carotid demonstrating low insertion of the left common carotid artery (L CCA) on the aortic arch. (b) 3D coronal reformat of CTA aortic arch and carotid demonstrating low insertion of the left common carotid artery (L CCA) on the aortic arch. Given challenging anatomy, patient was not take for EMMA. Left subclavian artery (L SCA), brachiocephalic artery (BCA). Given challenging anatomy, patient was not taken for EMMA.

https://doi.org/10.1017/cjn.2024.328 Published online by Cambridge University Press